Special Section
Mathematical and Computational Geophysics

Geofísica Internacional (2026) **65-3**: 2359- 2376

Assimilating chemical observations in the Mexico City Metropolitan Area using WRFDA-Chem

Gilberto Maldonado-Pacheco[1,a], Victor Almanza[1*,b], Luis Gerardo Ruiz-Suárez[1,c] and Agustín García-Reynoso[1,d]

Abstract

Air pollution exceedances are important air quality events for its associated effects on public health. Chemical transport models are frequently used for estimating pollution concentrations, especially in areas with limited monitoring capacity. Even though their performance may be improved by combining observations from different platforms through data assimilation, in Mexico these applications are limited, especially those aiming to assimilate chemical composition observations. In this study, surface observations of O_3, CO and NO_2 from the local monitoring network (RAMA) together with conventional global meteorological observations, were assimilated over the Mexico City Metropolitan Area (MCMA) using the WRFDA-Chem v4.5.2 assimilation system and the 3DVAR algorithm. The global observations were obtained in PREPBUFR format, and consisted of upper-air and surface weather reports collected worldwide. The observations included pressure, temperature, dew point, wind speed and direction, from several platforms including surface, radiosondes, and aircraft reports. Two sets of experiments focusing on the impact of the chemical initial and boundary conditions were conducted. One experiment used default chemical initial and boundary conditions provided. In the experiment denoted by "default", the WRF-Chem model was initialized through predetermined NALROM (NOAA Aeronomy Lab Regional Oxidant Model) ideal profiles that are included in the model. These profiles represent a northern-hemispheric, mid-latitude, relatively clean atmospheric composition and provide values for species such as O_3, CO, NO_x. (WRF-Chem user guide). The other experiment, denoted by "global", the NALROM ideal profile was replaced with external chemical fields obtained from the global chemical transport model WACCM (Whole Atmosphere Community Climate Model). These fields provide spatially and temporally varying initial and boundary conditions that reflect realistic large-scale chemical distributions rather than a static climatology. Results showed that chemical data assimilation corrected pollutants concentrations. Regarding CO and NO_2, differences between model results and observations were rather small, suggesting the need of tuning the background error covariance matrix parameters for these pollutants. However, for ozone, using global model outputs to initialize the model, tended to better represent regional maximum concentration, whilst using default conditions tended to better represent regional average concentration. However, both setups estimated similar daily ozone peaks. This suggests that using default chemical conditions cycled over a long period may optimize storage and computing resources.

Key words: WRFDA-Chem, data assimilation, air quality modeling, ozone.

Resumen

Las excedencias de contaminación atmosférica son eventos importantes de calidad del aire por sus efectos asociados en la salud pública. Los modelos de transporte químico se utilizan con frecuencia para estimar las concentraciones de contaminantes, especialmente en zonas con capacidad de monitoreo limitada. Si bien su rendimiento puede mejorarse combinando observaciones de diferentes plataformas mediante la asimilación de datos, en México estas aplicaciones son limitadas, especialmente aquellas que buscan asimilar observaciones de composición química. En este estudio, se asimilaron las observaciones en superficie de O_3, CO y NO_2 reportadas por red de monitoreo local (RAMA), junto con observaciones meteorológicas globales convencionales, en la Zona Metropolitana de la Ciudad de México (ZMCM) mediante el sistema de asimilación WRFDA-Chem v4.5.2 y el algoritmo 3DVAR. Las observaciones globales se obtuvieron en formato PREPBUFR y consistieron en informes meteorológicos de altitud y superficie recopilados a nivel mundial. Las observaciones incluyeron presión, temperatura, punto de rocío, velocidad y dirección del viento, provenientes de diversas plataformas, incluyendo informes de superficie, radiosondas y aeronaves. Se realizaron dos conjuntos de experimentos centrados en el impacto de las condiciones químicas iniciales y de frontera. Un experimento utilizó las condiciones químicas iniciales y de frontera predeterminadas. En el experimento "default", el modelo WRF-Chem se inicializó mediante perfiles ideales NALROM (NOAA Aeronomy Lab Regional Oxidant Model) predeterminados, incluidos en el modelo. Estos perfiles representan una composición atmosférica relativamente limpia en el hemisferio norte, en latitudes medias, y proporcionan valores para especies como O_3, CO y NO_x (Guía del usuario de WRF-Chem). En el otro experimento, "global", el perfil ideal NALROM fue reemplazado por campos químicos externos obtenidos del modelo global de transporte químico WACCM (Whole Atmosphere Community Climate Model). Estos campos proporcionan condiciones iniciales y de contorno que varían espacial y temporalmente, reflejando distribuciones químicas realistas a gran escala, en lugar de una climatología estática. Los resultados mostraron que la asimilación de datos químicos corrigió las concentraciones de contaminantes. En cuanto al CO y el NO_2, las diferencias entre los resultados del modelo y las observaciones fueron relativamente pequeñas, lo que sugiere la necesidad de ajustar los parámetros de la matriz de covarianza del error de fondo para estos contaminantes. Sin embargo, en el caso del ozono, el uso de las salidas del modelo global para inicializar el modelo tendió a representar mejor la concentración máxima regional, mientras que el uso de las condiciones predeterminadas tendió a representar mejor la concentración media regional. No obstante, ambas configuraciones estimaron picos diarios de ozono similares. Esto sugiere que el uso de condiciones químicas predeterminadas cicladas durante un período prolongado puede optimizar los recursos de almacenamiento y cómputo.

Palabras clave: WRFDA-Chem, asimilación de datos, modelación de la calidad del aire, ozono.

Received: May 18, 2025; Accepted: April 27, 2026; Published on-line: July 1, 2026. https://doi.org/10.22201/igeof.2954436xe.2026.65.3.1886

Editorial responsibility: Dr. Jorge Zavala Hidalgo, Universidad Nacional Autónoma de México, Instituto de Ciencias de la Atmósfera y Cambio Climático.

* Corresponding author: Victor Almanza, victor.almanza@atmosfera.unam.mx
[1] Universidad Nacional Autónoma de México, Instituto de Ciencias de la Atmósfera y Cambio Climático, Departamento de Química de la Atmósfera, Coyoacán, 04150, CDMX. México.
ORCID: [a]0009-0000-9659-6176, [b]0000-0002-4614-3205, [c]0000-0003-4159-1217, [d]0000-0001-7718-9241.

CC BY NC SA

1. Introduction

Air pollution is a problem that has intensified in recent years due to urban expansion, resulting in an increase in pollutant emissions. Pollution episodes (periods with high concentrations of pollutants) may last for several days and can impact public health, especially sensitive groups (INECC, 2024; WHO, 2024). These episodes coincide with low dispersion conditions, biomass burning activities, and high solar radiation, which altogether favor ground-level ozone production. In Mexico, they typically occur between February and May, during the so-called ozone season, and mainly affect Mexico City Metropolitan Area (MCMA) (INECC, 2020). However, the lack of surface observations in other metropolitan areas within the Megalopolis of Central Mexico, complicates monitoring these episodes at the regional level (Molina *et al.*, 2023). For this reason, analyzing these events could help identify their causes and contribute to developing control measures aimed at reducing pollution levels during episodes.

The complexity of atmospheric chemical reactions is influenced by emissions, transport, deposition, and chemical transformation. All these processes and their associated uncertainties impact model performance when estimating pollutants concentrations using chemical transport models (CTM) (Mallet & Sportisse, 2006; Aleksankina *et al.*, 2019). One approach to improve model performance consists in using observational data to constrain the model through data assimilation (DA). This technique aims to obtain a more accurate representation of the atmospheric state at a particular time. Traditionally, data assimilation has been mostly applied to meteorological forecasting in numerical weather prediction (Lee & Barker, 2005; Huang *et al.*, 2009). However, assimilation of chemical composition observations is a relatively more recent field and it has been used more frequently for air quality applications, including reactive gases and aerosol forecasting (Saide *et al.*, 2014; Bocquet *et al.*, 2015; Ha *et al.*, 2024).

Currently, there are several operational forecasting systems based on data assimilation worldwide. For example, the ECMWF/Copernicus Integrated Forecast system (IFS) developed in Europe, the Met Office UKV hourly 4D-Var system that has been operational since 2017 in the United Kingdom (Milan *et al.*, 2020), the DWD COSMO-KENDA and ICON-D2 global and regional numerical prediction systems, which have been operational since 2015 focusing on the European continent (Zängl *et al.*, 2015), and the NASA's GEOS-5 (Baklanov & Zhang, 2020) for global applications. Besides, a few examples of operational forecasting systems based on chemical data assimilation are CAMS (Copernicus Atmosphere Monitoring Service) system developed by ECMWF for global applications of both gas and aerosols (Peuch *et al.*, 2022), MERRA-2 (Modern-Era Retrospective analysis for Research and Applications Version 2) developed by NASA for global application focusing on aerosols (Gelaro *et al.*, 2017) and the WRF-Chem/DART regional system (Mizzi *et al.*, 2016).

In Mexico, the number of published studies related to data assimilation is limited and mostly have focused on the assimilation of meteorological variables (Yang *et al.*, 2017; Risanto *et al.*, 2021). In addition, previous studies related to air quality applications have applied only meteorological data assimilation with the objective of improving modeled pollutant concentrations. For example, between 2008 and 2012, studies applied different techniques to assimilate meteorological variables (Bei *et al.*, 2008; 2010; 2012) with the aim of enhancing chemical simulations, particularly ozone and secondary organic aerosol (SOA) concentrations in Mexico City. Later, Bei *et al.*, (2014) analyzed the impact of using the Ensemble Kalman Filter in air quality simulations in the California-Mexico border area during the Cal-Mex field campaign to improve ozone concentration. More recently, Martínez-Sabari & García-Reynoso (2021) evaluated the impact of assimilating meteorological variables on ozone concentration in the MCMA using the 3DVAR assimilation technique. Chemical data assimilation (CDA) has not yet been implemented in Mexico and could become a key tool to enhance air quality model performance. To the best of our understanding this is the first application in Mexico of online chemical data assimilation using variational methods with WRFDA-chem.

The objective of this study is to present a sensitivity analysis of the WRFDA-Chem system for the MCMA under different initial and boundary conditions when assimilating ozone (O_3), carbon monoxide (CO) and nitrogen oxide (NO_2) surface observations. In this sense, this work may contribute to the ongoing effort of enhancing the forecasting capability of CTM in Mexico through data assimilation of reported criteria pollutants.

This work is organized as follows. Section 2 presents a description of the WRFDA- Chem assimilation system, including the WRF-Chem configuration and WRFDA assimilation requirements. Section 3 presents the numerical experiments conducted for sensitivity analysis. Modeling results and model evaluation are also discussed. Finally, conclusions are summarized in Section 4.

2. Data and Methods

2.1. WRFDA-Chem system

In this study WRFDA-chem is employed to conduct chemical data assimilation (CDA) over the Mexico City Metropolitan Area (MCMA). This system was developed recently with the aim of ingesting surface observations from monitoring networks and couples the WRFDA assimilation system with the WRF-Chem air quality model (Sun *et al.*, 2020; Ha, 2022). The main components are briefly described as follows.

2.1.1. WRF-Chem

The Weather Research Forecast Model coupled with Chemistry (WRF-Chem) model (Grell *et al.*, 2005) is a mesoscale regional online chemistry transport model that was developed as a collaborative effort of different research centers led by the Global Systems Laboratory (GSL, NOAA) and the National Center for Atmospheric Research (NCAR). It is capable of jointly simulating meteorological fields, emissions from anthropogenic sources, biomass burning activities and chemical species concentrations using an available set of chemical mechanisms.

In this study, WRF-Chem v4.5.2 with the RACM/MADE VBS chemical mechanism was used to simulate ozone (O_3), carbon monoxide (CO) and nitrogen dioxide (NO_2) concentrations.

2.1.2. WRFDA

The Weather Research and Forecast Data Assimilation (WRFDA) is an assimilation system that combines observations, modeled data and their associated errors to improve model estimations (Barker *et al.*, 2012). Different DA algorithms have been implemented in this assimilation system such as the Three-dimensional variational assimilation (3DVAR), the Four-dimensional variational assimilation (4DVAR), and their respective hybrid options (3DEnVAR and 4DEnVAR) that make use of ensemble background errors within a variational framework (Vendrasco *et al.*, 2016; Ban *et al.*, 2017; Davis *et al.*, 2021; Yang & Wang, 2024).

In this study we used WRFDA-Chem v4.5.2 to assimilate meteorological and chemical observations with the 3DVAR variational algorithm that estimates the optimal combination with the modeled variables (analysis) through a minimization process of a cost function represented by *J(x) (equation 1)*:

$$J(x) = \frac{1}{2}(x - x_b)^T B^{-1} (x - x_b) + \frac{1}{2}(H(x) - y)^T R^{-1} (H(x) - y) \quad (1)$$

where $\boldsymbol{x_b}$ is the background field vector, $\boldsymbol{y}$ is the observation vector, $\boldsymbol{H}$ is the observation operator that converts the model state to the observed quantities, and $\boldsymbol{B}$ and $\boldsymbol{R}$ represent the background error and observation error covariance matrices respectively.

This system has the capability of assimilating meteorological variables from surface networks, radars, buoys, ships, and other observational platforms. On the other hand, WRFDA-chem was developed based on WRFDA to ingest chemical composition observations at ground level. Currently this chemical data assimilation system has the capability to process surface observations of 6 chemical species, 4 in gas phase (SO_2, NO_2, O_3 and CO) and 2 in particulate phase ($PM_{2.5}$, PM_{10}) (Sun *et al.*, 2020; Ha, 2022). In addition, it only supports GOCART (Chin *et al.*, 2000), MOSAIC (Zaveri *et al.*, 2008) and RACM/MADE-VBS (Stockwell *et al.*, 1997; Ahmadov *et al.*, 2012) chemical mechanisms (Ha, 2022).

One of the main reasons for using the 3DVAR algorithm is that although its limitations such as using a static background error covariance and a linearized forecast model, its computational time is feasible for operational settings related to air quality (Ha, 2022). The expensive computations required for solving stiff chemical mechanisms with hundreds of prognostic variables is a parameter to be accounted for when considering the implementation of an operational forecasting with limited resources. Using 3DVAR lets us optimize computational resources compared to 4DVAR due to the extra computational cost required to solve the adjoint and tangent-linear models in the four-dimensional variational assimilation technique.

2.1.2.1. Background error

The background error covariance matrix (**B**) was estimated using the GEN_BE 2.0 software (Descombes *et al.*, 2015), which modifies the original GEN_BE (included in the WRFDA system) to process chemical observations. This tool allows the estimation of several statistics for meteorological variables as well as chemical species; such as the standard deviation, vertical and horizontal length scales, and vertical correlations. Currently, it supports different aerosols mechanisms such as MADE-VBS, GOCART and MOSAIC.

In this study, **B** was calculated for each domain using the National Meteorological Center (NMC) method (Parrish & Derber, 1992) with 12h and 24h WRF-Chem forecasts valid at the same time from March 22 to 29, 2023.

2.2. Emissions

Emissions data from the 2016 Mexican National Emissions Inventory (SEMARNAT, 2019) was processed for modeling by using the Spatial, Temporal and Speciation Distribution Model (DiETE) (García-Reynoso *et al.*, 2018) in order to prepare model-ready files with the RACM chemical mechanism speciation.

Emissions of volatile organic compounds (VOCs) and nitrogen oxides (NOx) were scaled for the modeling period with the objective to better represent O_3, NO_2 and CO concentrations to surface observations due to the uncertainty associated with the estimation of emissions (West *et al.*, 2004; Lei *et al.*, 2007).

2.3. Observations

Global observations were obtained in PREPBUFR format, which are generated operationally by NCEP and consisted of upper-air and surface weather reports collected worldwide. The observations included pressure, temperature, dew point, wind speed and direction, from several platforms including surface, radiosondes, and aircraft reports (NCEP, 2025b). Important to highlight is the scarce number of available data over Central Mexico, which is about 1 station close to the MCMA on March 31st at 18:00 UTC (Figure 1).

In addition, O_3, CO and NO_2 surface measurements reported by the Mexico City local monitoring network (RAMA) (SEDEMA, 2025) were employed to assimilate pollutants concentrations (Figure 2). This monitoring network covers Mexico City and part of State of Mexico and is hosted by the Environmental Secretariat. It reports hourly observations of criteria pollutants (ozone, carbon monoxide, nitrogen oxides, sulfur dioxide and particulate matter) and meteorological variables (temperature, relative humidity, wind speed and wind direction). It began operations in 1986 and currently operates with more than 30 stations and are publicly available as 1-h averages after being validated following the US Environmental Protection Agency standards (SEDEMA, 2025).

2.4. WRF-Chem model configuration

In this study, the WRF-Chem model was forced with the meteorological Global Forecast System at 0.25° resolution from NCEP (NCEP, 2025a) and configured with two nested domains. The outer domain consisted of a 215 by 150 cells with 15 km resolution, while the inner domain comprised a 96 by 63 cells grid with 5 km resolution (Figure 3). Additionally, an updated 30" resolution urban coverage dataset for the MCMA (López-Espinoza *et al.*, 2012) was employed.

The following parameterizations were used to simulate physical processes occurring in the atmosphere: 1) the YSU scheme for the boundary layer (Hong *et al.*, 2006); 2) the WSM6 (WRF Single-Moment 6-class) option for microphysical processes (Hong & Lim, 2006); 3) the Rapid Radiative Transfer Model (RRTM) for processes related to shortwave and longwave radiation (Iacono *et al.*, 2008); and 4) the Grell-3D ensemble scheme for the convection (cumulus) option (Grell, 1993; Grell & Dévényi, 2002).

The modeling period spans from March 31st to April 3rd, 2023, with 1 day of spin-up. The criteria to select this period were: 1) meteorological conditions without much influence of synoptic-scale phenomena (cold fronts) (CONAGUA, 2024); 2) negligible fire emissions from biomass burning activities (CONAFOR, 2024); 3) no additional emissions adjustment. The mobility restrictions associated with the COVID-19 lockdown ended in Mexico in late 2022, so that a modeling period in 2023 was preferred.

2.5. Experiment design

In this study, WRF-Chem and WRFDA cycling experiments were conducted from March 31st to April 3rd, 2023, every 6 hours for forecast and assimilation cycles, with one day of spin-up in a WRF-Chem one-way nesting configuration (Table 1). Since one of the aims of data assimilation is to improve the initial state of

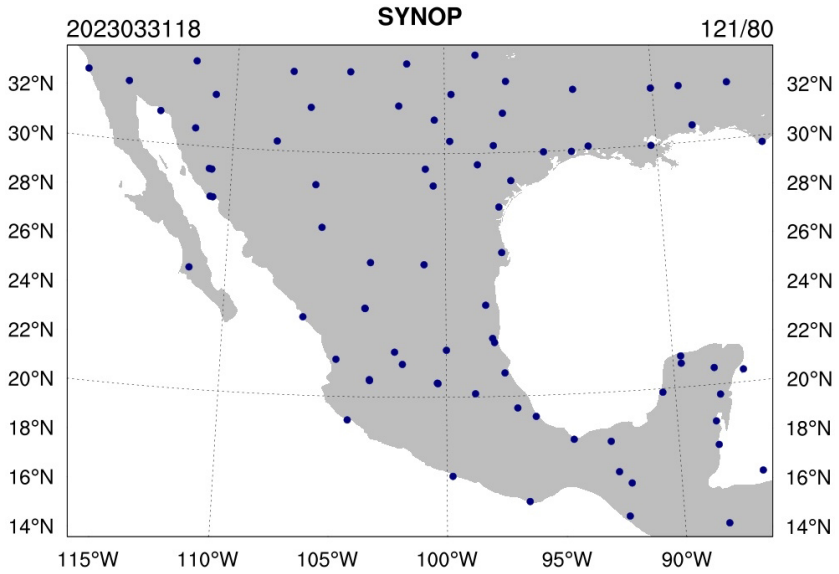

Figure 1. Available synoptic stations on March 31st at 18:00 UTC in NCEP PREPBUFR dataset.

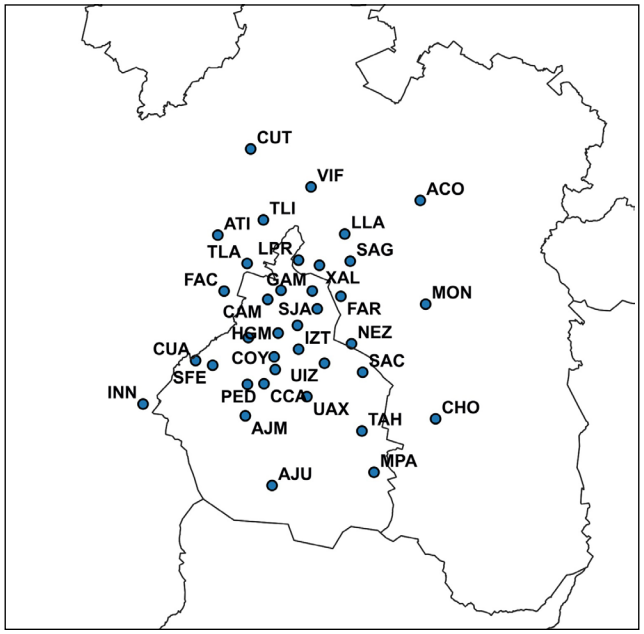

Figure 2. RAMA surface monitoring network in MCMA.



Figure 3. Modeling domains at 15 km (black) and 5 km (blue) resolution.

a model, a total of two numerical experiments focusing on the impact of the chemical initial and boundary conditions were considered. One experiment used the default (DFLT) chemical conditions provided by the WRF-Chem model through the NALROM (NOAA Aeronomy Lab Regional Oxidant Model) ideal profile (McKeen *et al.*, 2002). The other experiment used chemical conditions provided by a separate global chemical transport model (GLOB). For this case, outputs from the Whole Atmosphere Community Climate Model (National Center for Atmospheric Research, 2026.) (WACCM) was used. The meteorological initial conditions were kept the same in all experiments because analyzing the coupled impact of chemistry and meteorology is beyond the scope of this study.

These numerical experiments were designed considering a limited computational resources framework. For this reason, choosing how to solve the stiff chemical mechanism was very important. Two approaches were considered. One approach consisted on solving the chemistry only in the innermost

domain, which implies to firstly run the outer domain and then run separately the innermost domain. The advantage of this approach is that there is no need to solve the chemistry at the national level, which is computationally intensive. The second approach consisted of running the chemistry in both domains, which means running the model in a 1-way simultaneous run and solving the chemistry at both the national level (domain one, D01) and the regional level (domain two, D02). The workflow of both approaches is described as follows.

D01_NoDA simulation was carried out for the outer domain without data assimilation and chemistry turned off. Meteorological fields from the first cycle were used to initialize the next cycle and so on. In addition, meteorological initial and boundary conditions from GFS (Global Forecast System) were updated in every 6-hour cycle. Then, the control experiment (NoDA-chem) was carried out without data assimilation and chemistry turned on. Initial and boundary conditions were provided from D01_NoDA experiment through a one-way nesting setup. Besides, similar to meteorological variables, the chemical fields from the first cycle were used to initialize the next cycle and so on.

The D02_DFLT experiment was performed with assimilation of O_3, CO and NO_2 surface observations from RAMA network. As mentioned before, the initial and boundary conditions were carried over from D01_D_ICBC simulation based on the ideal NALROM profile. The difference with respect to the D02_GLOB experiment is that the initial and boundary conditions were generated from D01_G_ICBC simulation using WACCM model outputs. In both D01_ D_ICBC and D01_G_ICBC experiments, meteorological observations (temperature (T), relative humidity (RH), wind components (U, V) and pressure (P)) were assimilated by employing global data in PREPBUFR format (NCEP, 2025b).

Subsequently, the quality of the assimilation was evaluated using metrics such as the observation minus background (OMB), observations minus analysis (OMA), and increments (difference between analysis and background). OMB is calculated using prior information (i.e. before assimilation) and OMA is estimated *a posteriori* (i.e. employing the DA outcome). Therefore, the magnitude of OMA should be smaller than OMB if the assimilation is working properly (Ha, 2022).

Model evaluation was estimated using traditional statistical metrics, like the index of agreement (d) (Willmott *et al.*, 1985), the root mean square error (RMSE) and the Pearson correlation coefficient.

3. Results and Discussion

The results presented in this section will consider two aspects. First, evaluating the quality of the assimilation using the observation minus background (OMB), observation minus analysis (OMA) and the increments. Second, evaluating the impact of the assimilation on model performance employing both the regional hourly average and regional hourly maximum concentrations of O_3, CO and NO_2 based on 34 RAMA monitoring stations. All the presented results in this section correspond to the inner domain (D02).

Table 1. Simulation experiments and their main settings.

Domain	Experiment	Meteorological or chemical variables assimilated	Assimilated time (UTC)	Simulation features
	D01_NoDA	None	-	Default chemical initial and boundary conditions. Chemistry turned off.
Outer domain (D01)	D01_ D_ICBC	T, U, V, RH, P	00:00, 06:00, 12:00, 18:00	Default chemical initial and boundary conditions. Chemistry turned off.
	D01_ G_ICBC	T, U, V, RH, P	00:00, 06:00, 12:00, 18:00	Chemical Initial and boundary conditions from WACCM model. Chemistry turned on.
	NoDA-chem	None	-	Control experiment. Chemistry turned on
Inner domain (D02)	D02_DFLT	O_3, CO, NO_2	00:00, 06:00, 12:00, 18:00	Default chemical initial and boundary conditions from outer domain (D01_ D_ICBC)
	D02_GLOB	O_3, CO, NO_2	00:00, 06:00, 12:00, 18:00	Global chemical initial and boundary conditions from outer domain (D01_ G_ICBC)

3.1. Assimilation quality

Figure 4 shows time series of the observation minus background (OMB) and the observation minus analysis (OMA) in terms of the RMSE for O_3, CO and NO_2 for the simulation period. With respect to O_3 the OMA tended to be smaller than the OMB for both DA experiments (D02_DFLT and D02_GLOB) which means that data assimilation tended to correct the model concentration. On the other hand, for both CO and NO_2 the OMA was lower than the OMB in some assimilation cycles for both DA experiments, but no significant changes were found associated with the use of different initial and boundary conditions. On the contrary, in other assimilation cycles (for example on 2023-03-31 06:00 UTC, 2023-04-01 12:00 UTC or 2023-04-02 12:00 UTC) both RMSE magnitudes of OMB and OMA were very similar to each other. This indicates that the assimilation had a small impact on modeled concentrations at these hours.

Figures 5 and 6 show the horizontal distribution of average analysis increments (obtained as the difference between the analysis minus the background) in the assimilated variables (O_3, CO, and NO_2) for both DA experiments. D02_DFLT (upper row) and D02_GLOB (bottom row). These increments correspond to the lowest model level, averaged at 00:00 UTC and 18:00 UTC assimilation cycles for the simulation period.

The 00:00 UTC hour was selected because it is important for representing fresh emissions linked to early-morning mobile emissions in the MCMA. Conversely, the 18:00 UTC period was selected because it represents the increase in ozone concentration, reflecting photochemical processes that occur during daylight hours.

At 00:00 UTC, average ozone concentration was increased to southeast of MCMA using the default initial and boundary conditions, indicating that it was underestimated in the background forecasts (upper row). On the contrary, it was reduced to the northwest of MCMA suggesting that the O_3 concentration was overestimated in the background concentration. However, when using the global chemical conditions, ozone concentration was reduced in all the MCMA (bottom row). This suggests that the

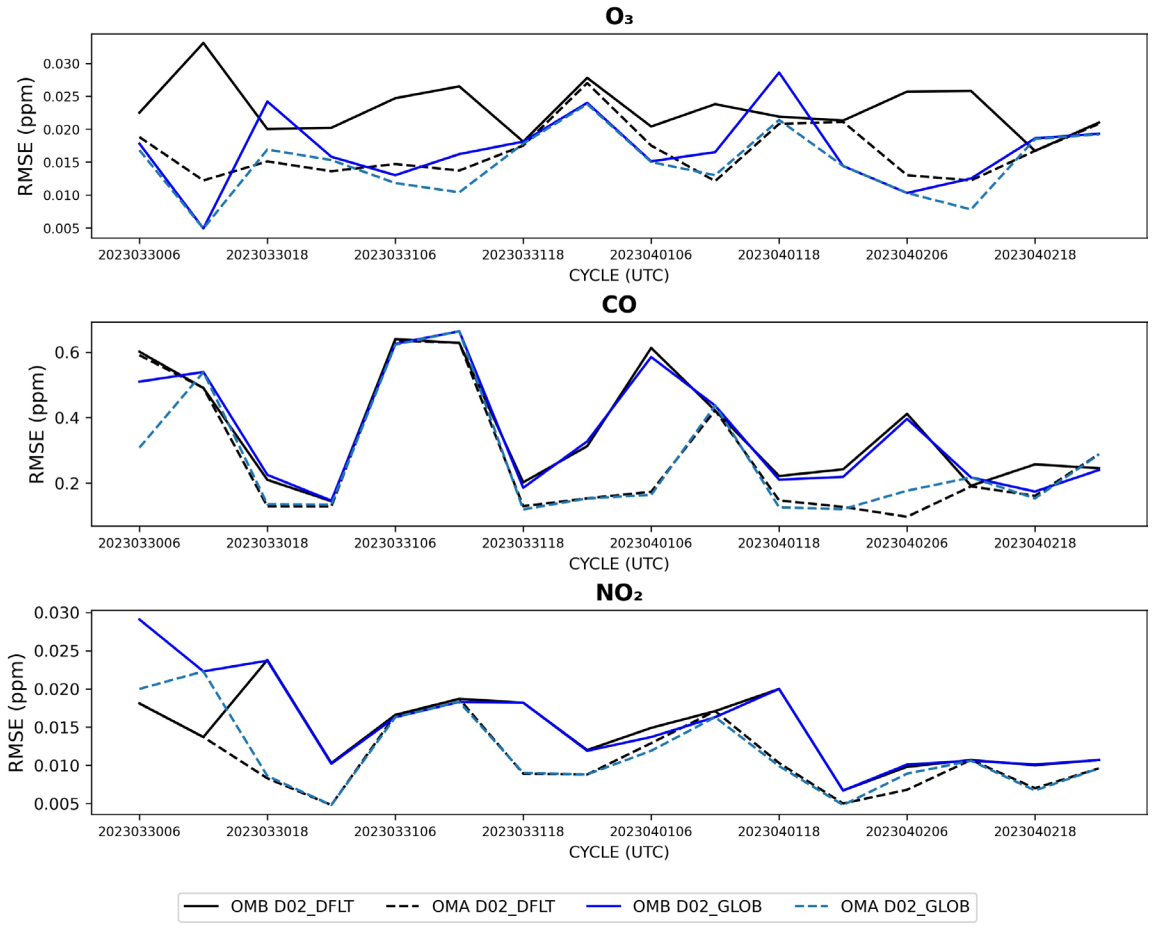

Figure 4. Time series of observation minus background (OMB, solid lines) and observation minus analysis (OMA, dashed lines) at each assimilation cycle in terms of root-mean-square error. Black line denotes D02_DFLT experiment and blue line denotes D02_GLOB experiment.

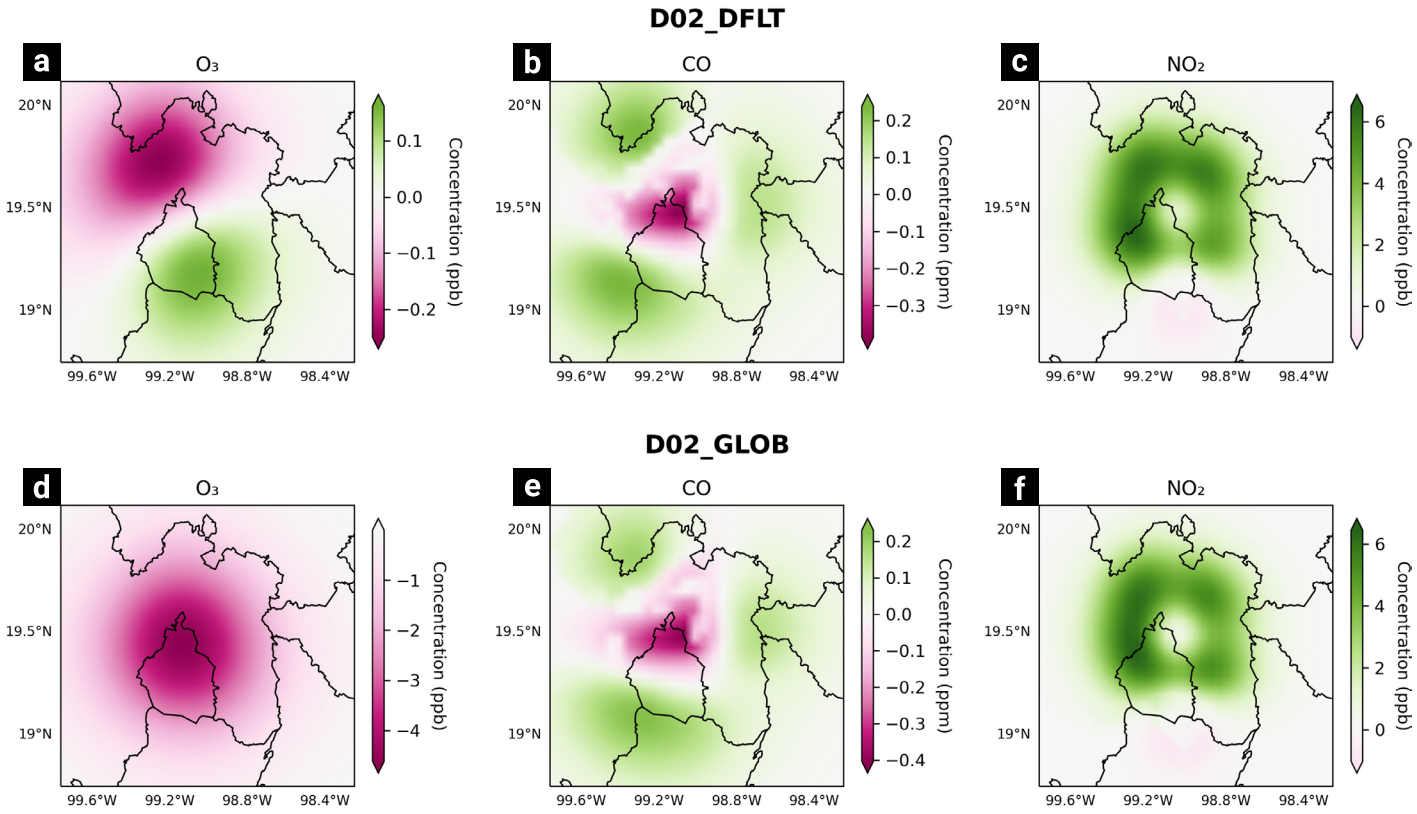

Figure 5. Horizontal distribution of the analysis increments for O_3, CO and NO_2 averaged at 00:00 UTC assimilation cycles.

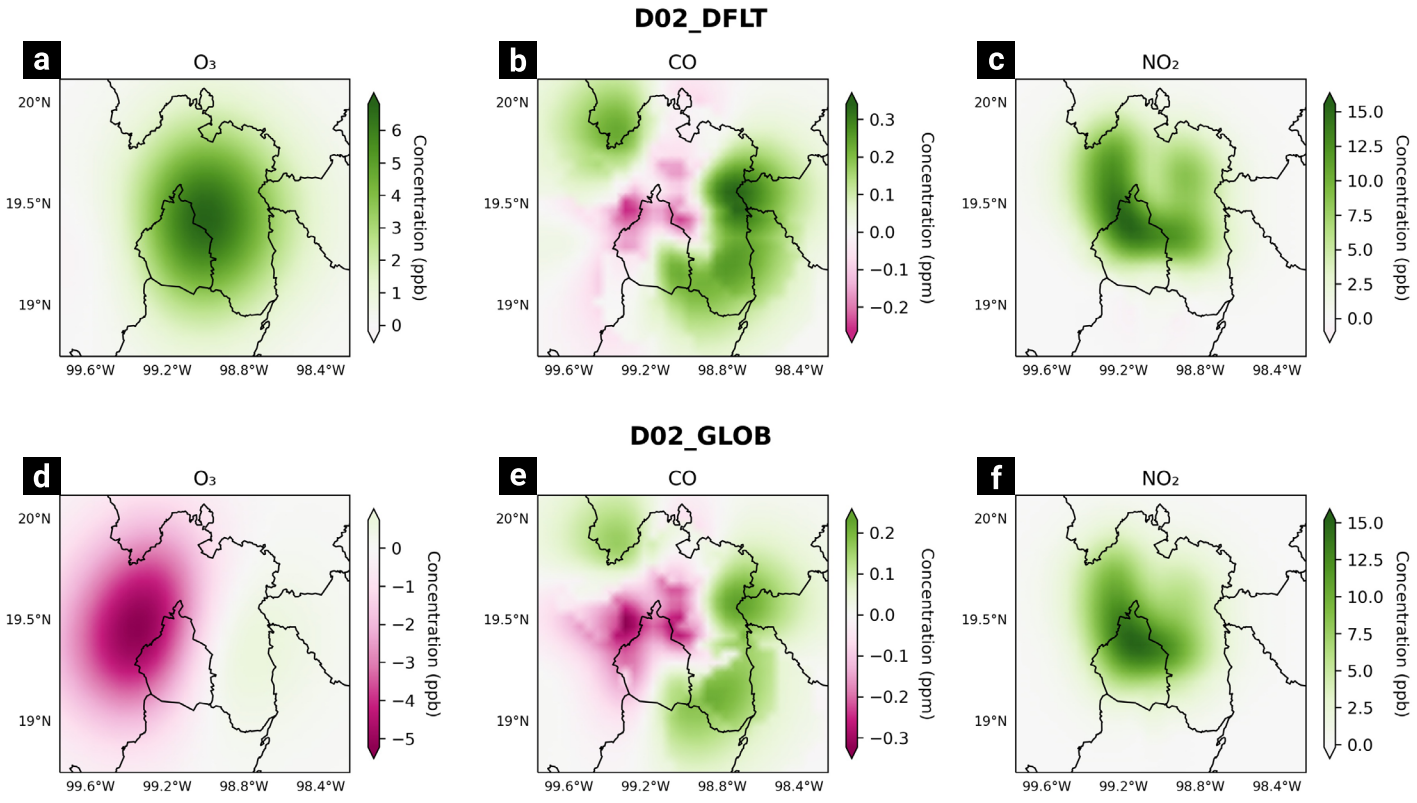

Figure 6. Horizontal distribution of the analysis increments for O_3, CO and NO_2 averaged at 18:00 UTC assimilation cycles.

background ozone level in the global model is higher than the default chemical conditions. In addition, CO concentrations increased in the periphery of MCMA but decreased in the center area in both DA experiments. This implies that CO background concentration was underestimated around the MCMA center whereas it was overestimated on the outskirts of this metropolitan region. Finally, NO_2 concentrations augmented in most of MCMA in both DA experiments. This means that the background concentration was increased in order to approximate model results to observations.

These results illustrate that integrating chemical surface observations into the model may help diminish differences between modeled and observed concentrations data likely driven by the uncertainty in the emission inventory. Likewise, it is shown that for O_3 and CO concentrations, their concentrations increased in some areas but in contiguous regions they decreased. This may be related to the uncertainty in the estimation of ozone precursors (VOCs and NOx) and CO emissions in the emission inventory. Furthermore, the magnitudes of the increments and the impacted area are similar using default and global chemical conditions (D02_DFLT and D02_GLOB experiments, respectively) for CO and NO_2 which indicate that the use of different initial and boundary conditions did not have an impact on their concentrations at 00:00 UTC. However, it is worth investigating for an extended period.

At 18:00 UTC, average ozone concentration was primarily enhanced all over the MCMA when using default chemical conditions (D02_DFLT experiment). However, similar to the 00 UTC, the concentration was reduced mostly over the northern and western areas of the MCMA when using global chemical conditions (D02_GLOB case). These results may be related to the underestimation in D02_DFLT and an overestimation in D02_GLOB in the model background concentration possibly because its precursors emissions are likely not well represented in the emission inventory.

Regarding CO, the magnitudes of the increments were significantly different in both experiments probably as a result of different background concentrations (corrected by assimilation in previous cycles) and distinct initial and boundary conditions.

With respect to NO_2, an increase in its concentration was suggested in both DA experiments, most likely related to underestimated emissions in the emissions inventory; therefore, its concentration was underestimated in the model background concentration and a correction was needed through the assimilation process. Furthermore, no significant difference was observed when using default and global initial and boundary conditions. This means that background concentrations were similar for both DA experiments suggesting that the magnitude of the assimilation correction was comparable in both DA experiments.

Figure 7 illustrates the vertical profiles of the average increments O_3, CO and NO_2 estimated at a point within MCMA (lat=19.1, lon -99). These profiles characterize the magnitude and vertical distribution of the adjustments performed by the assimilation system for both DA experiments (D_ICBC and G_ICBC) at two key synoptic hours (00z and 18z).

The O_3 profiles showed different sensitivity patterns depending on times of day and experiments configurations

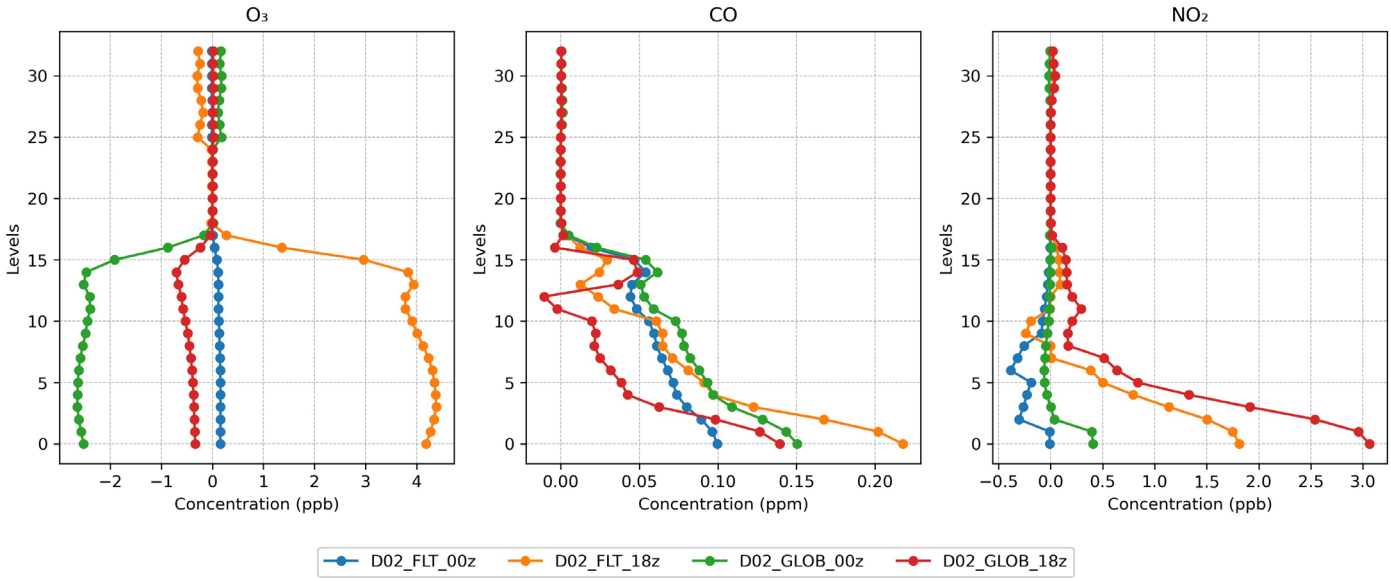

Figure 7. Average vertical profiles of the assimilation increments (analysis minus first guess) at a point located within the ZMVM (lat=19.1, lon -99) for O_3 (ppb), CO (ppm), and NO_2 (ppb) obtained from WRFDA-Chem. The profiles compare the D_ICBC and G_ICBC configurations at 00z (blue and green) and 18z (orange and red) over the study period.

within the lower troposphere (levels 0 to 17). In this sense, the D02_FLT_18z configuration (orange) shows significant positive increments, peaking at approximately 4 ppb near surface. Considering that the increment is equal to the difference between analysis and background, this result indicates that the first guess underestimated the O_3 concentrations compared to the assimilated observations. Conversely, the D02_GLOB_00z profile (green) exhibits a substantial negative reduction of about 2.5 ppb suggesting that the DA system reduced the O_3 concentrations to correct the bias in the first guess. Above level 20, the increments for all experiments converge toward zero, indicating that the impact of the assimilated surface data is primarily confined to the planetary boundary layer (PBL).

The CO profiles exhibit positive corrections across all DA experiments in the lowest 10 levels, but the largest adjustment occurs in the D02_FLT_18z experiment, with an increment exceeding 0.20 ppm at surface. This suggests an underestimation of CO concentration in the first guess, potentially due to low CO emissions or insufficient vertical transport near the surface. Moreover, all increments decrease monotonically with height, reaching near-zero values at level 17. This vertical structure suggests that the DA system corrected CO concentration mostly within the PBL.

NO_2 corrections are localized to the lowest levels (0-10), consistent with the short atmospheric lifetime of this species. Besides, significant adjustments are observed at 18z (orange and red lines), with the D02_GLOB_18z experiment showing the highest positive increment (approximately 3 ppb) at surface which implies a first guess underestimation of NO_2 observations. At 00z, the increments for both D02_FLT and D02_GLOB are close to zero or slightly negative, suggesting that the first guess is more accurately aligned with observations.

Figures 8 and 9 illustrate the analysis statistics of O_3 averaged at 00:00 UTC and 18:00 UTC assimilation cycles for D02_DFLT and D02_GLOB experiments. Ozone was chosen for this discussion because pollution episodes frequently occur due to high concentrations of this pollutant.

At 00:00 hours the model performance was better in the D02_DFLT experiment. However, the spread of the data suggests that the background concentration had a small correction in both DA experiments since RMS and standard deviation slightly decreased (Figure 8). Consequently, further investigation is required to improve model performance. For example, the assimilation of meteorological and chemical variables simultaneously in the inner domain, since in this study meteorological data assimilation was considered just for the outer domain.

At 18:00 UTC the magnitude of the correction through data assimilation was greater than at 00:00 UTC. It is observed that the model performance was best for the D02_GLOB experiment on account of the lower magnitudes of statistical metrics (RMS around 19 and 15 respectively) (Figure 9). However, tuning the assimilation parameters in WRFA-Chem system will likely improve model performance. This will be explored in a future study.

These results also imply that additional research about the impact of the background and observation error covariance matrices in the analysis estimation is needed given that the solution of the minimization of the cost function (equation 1) depends on these terms. Excessively small values of B (background error covariance matrix) could lead to *J* being predominantly dependent on the term associated with model estimations, and vice versa.

3.2. Model evaluation

Figure 10 shows time series comparing the hourly regional average of all monitoring stations within the MCMA for the two DA experiments in the inner domain and the control (NoDA_chem) experiment. Compared to NoDA_chem experiment (blue line), the chemical data assimilation (red and green lines) improves hourly average estimations for O_3 with closer values to observed peaks for the D02_GLOB (red line). However, using default chemical conditions tended to better approximate evening and early morning ozone concentrations. As for CO, we found that during the first two days the three experiments showed similar concentrations at peaks values, but their magnitudes were lower than the observations. Besides, the minimum values were overestimated in the DA experiments. With respect to NO_2, the assimilation improved the model performance during the first 12 hours of March 31st but in the following assimilation cycles estimations were lower than the measurements and closer to the control experiment. This implies that the assimilation system is discarding observations that even though they might correct the model concentration estimation, they are instead being considered as outliers based on strict thresholds.

Furthermore, despite that the average increments were greater than 4 ppb for O_3, 6 ppb for NO_2 and 0.4 ppm for CO at 00:00 UTC (Figure 5), these changes were not directly reflected in the concentrations, particularly for CO and NO_2. This could be explained by a degraded model performance in terms of meteorology, requiring improvements in the estimation of temperature, wind direction, wind speed or relative humidity through the assimilation of meteorological data within the study domain. As previously mentioned, there is just one synoptic station over the MCMA area (Figure 1) and most of the time there is only one radiosonde data available during the day. Thus, it is likely that the impact of a single observation is impacting a wide region. Since the MCMA is located in complex terrain, this impact might not be representative for an entire region, neither in the horizontal extent nor in the vertical extent, because it may also be

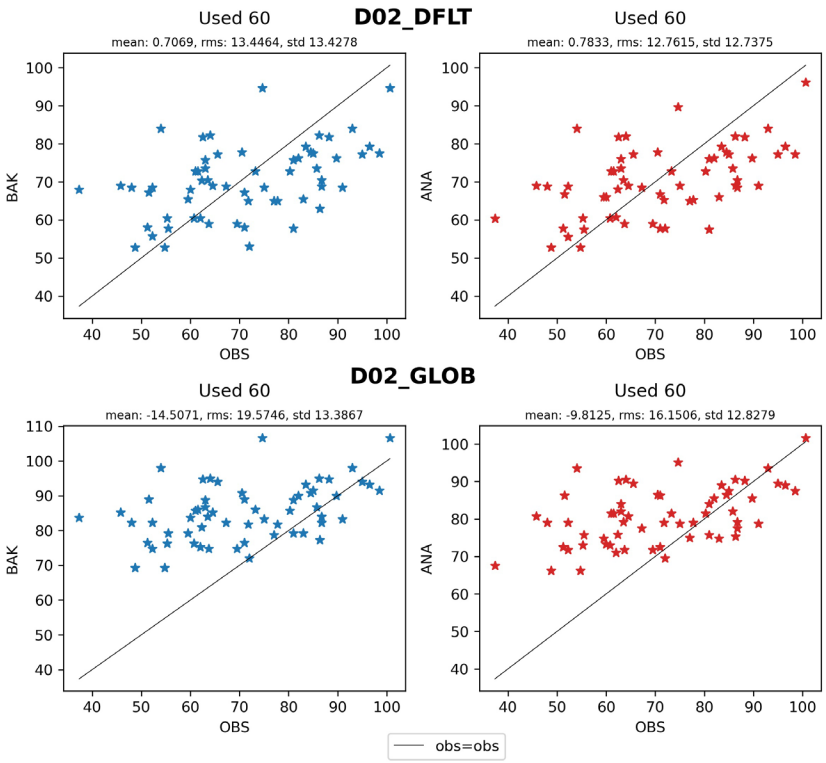

Figure 8. Averaged scatterplot of observation versus background (BAK, left column) and observation versus analysis (ANA, right column) for O_3 at 00:00 UTC. The top plots show results for D02_DFLT and bottom plots for D02_GLOB. The numbers above each panel denote numbers of the observations used in the assimilation process.

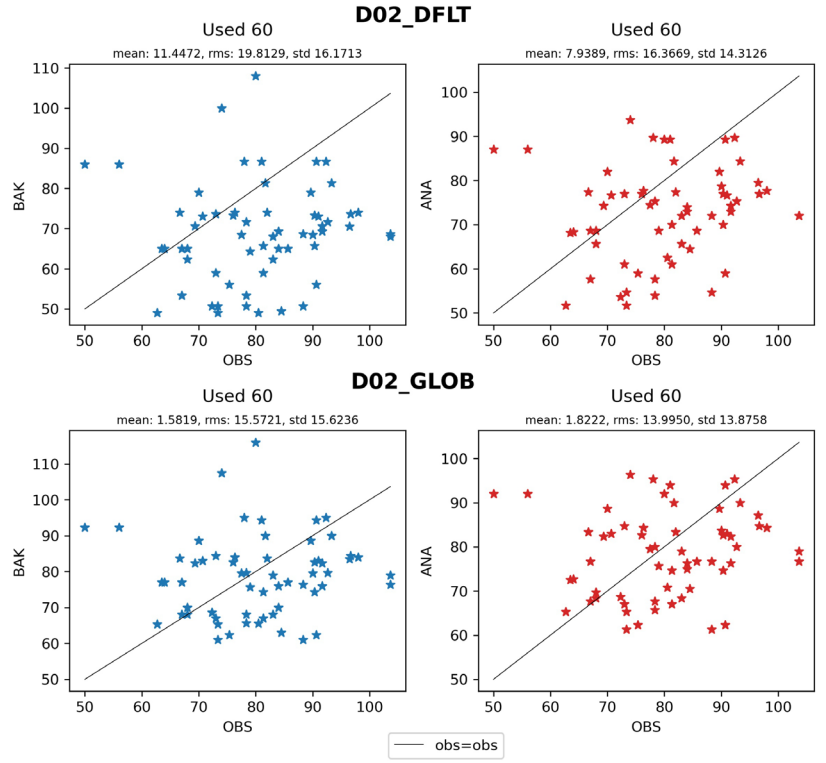

Figure 9. Averaged scatterplot of observation versus background (BAK, left column) and observation versus analysis (ANA, right column) for O_3 at 18:00 UTC. The top plots show results for D02_DFLT and bottom plots for D02_GLOB. The numbers above each panel denote numbers of the observations used in the assimilation process.

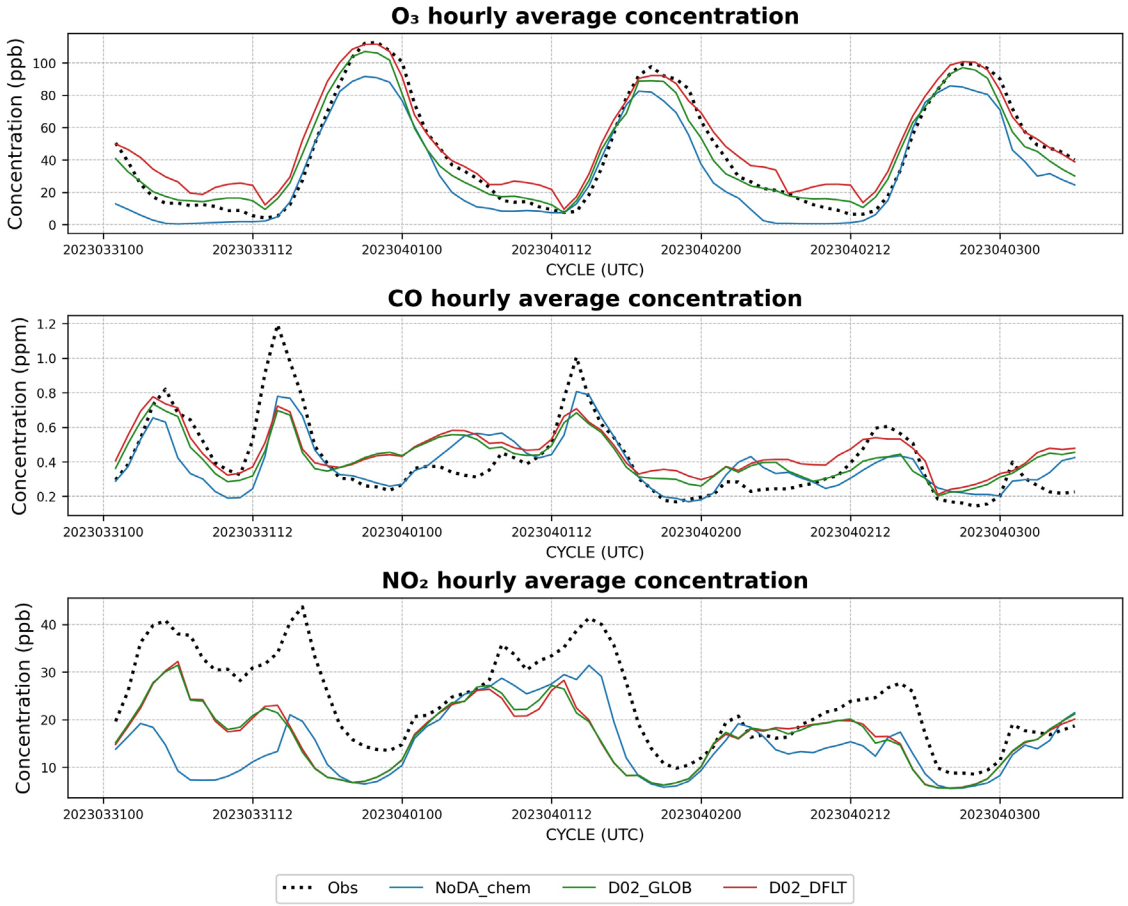

Figure 10. Time series of O_3, CO and NO_2 comparing observed (dots) and modeled hourly regional average concentrations for the NoDA_chem (blue), D02_GLOB (green) and D02_DFLT (red) experiments.

impacting the boundary layer as resolved by the model. Thus, in a future study, meteorological surface data from RAMA and the National Weather Service will be considered in the assimilation. Additionally, adjusting assimilation parameters in the background error covariance matrix (variance, length scale, among others) could enhance model performance for both chemical and meteorological variables.

Table 2 shows the model evaluation for the control case and D02_DFLT and D02_GLOB experiments using the hourly average concentration for O_3, CO and NO_2 concentrations. In addition, even though the main objective of this study is to evaluate the model performance for chemical species, statistical metrics for temperature (T), relative humidity (RH), zonal wind component (U) and meridional wind component (V) are presented just for completeness, with the aim of having a complete overview of all aspects that affect the concentration of pollutants.

It is observed that the DA experiment improved the average modeled concentrations of O_3 and NO_2, finding the best performance for the D02_DFLT experiment. Conversely, the model performance slightly decreased for CO in the DA experiments. Important to mention, is that statistical metrics for meteorological variables did not change in both DA experiments, because WRFDA-chem does not allow that meteorological state variables impact the chemical state variables in the assimilation step. In addition, there were few meteorological observations available for assimilation in the modeling domain (Figure 1).

Time series using hourly maximum concentrations are also presented due to the importance that maximum ozone concentrations have on pollution episodes in MCMA. In this sense, Figure 11 depicts time series comparing the hourly regional maximum of all monitoring stations within the MCMA for the NoDA_chem (blue), D02_DFLT (green) and D02_GLOB (red) experiments.

With respect to O_3, hourly maximum estimations for both D02_GLOB and D02_DFLT were closer to the peak observed values compared to the control experiment without data assimilation. Similar to the hourly average concentration time series, assimilating chemical observations improved the modeled ozone during the late evening and early morning hours. Regarding CO, these results showed a slight improvement in early hours and also at the estimation of the lowest maximum values, but modeled concentrations didn't reach the peak value on April 1st 12:00 UTC, April 2nd 12:00 UTC and April 3rd 00:00 UTC cycles. As

Table 2. Statistical metrics using hourly regional average concentrations for NoDA_chem, D02_DFLT and D02_GLOB experiments.

		NoDA_chem	D02_DFLT	D02_GLOB
O_3	d	0.83	0.92	0.85
	RMSE	10.72	5.92	10.35
	Pearson	0.99	0.99	0.98
CO	d	0.71	0.58	0.55
	RMSE	0.13	0.14	0.14
	Pearson	0.74	0.64	0.73
NO_2	d	0.28	0.38	0.38
	RMSE	9.00	8.25	8.21
	Pearson	0.96	0.85	0.87
T	d	0.90	0.89	0.89
	RMSE	1.09	1.18	1.18
	Pearson	0.99	0.99	0.99
RH	d	0.92	0.87	0.87
	RMSE	2.71	4.52	4.54
	Pearson	0.99	0.99	0.99
U	d	-0.18	-0.33	-0.33
	RMSE	1.36	1.60	1.61
	Pearson	-0.66	-0.89	-0.89
V	d	-0.09	-0.21	-0.21
	RMSE	1.58	1.63	1.63
	Pearson	-0.27	0.23	0.22

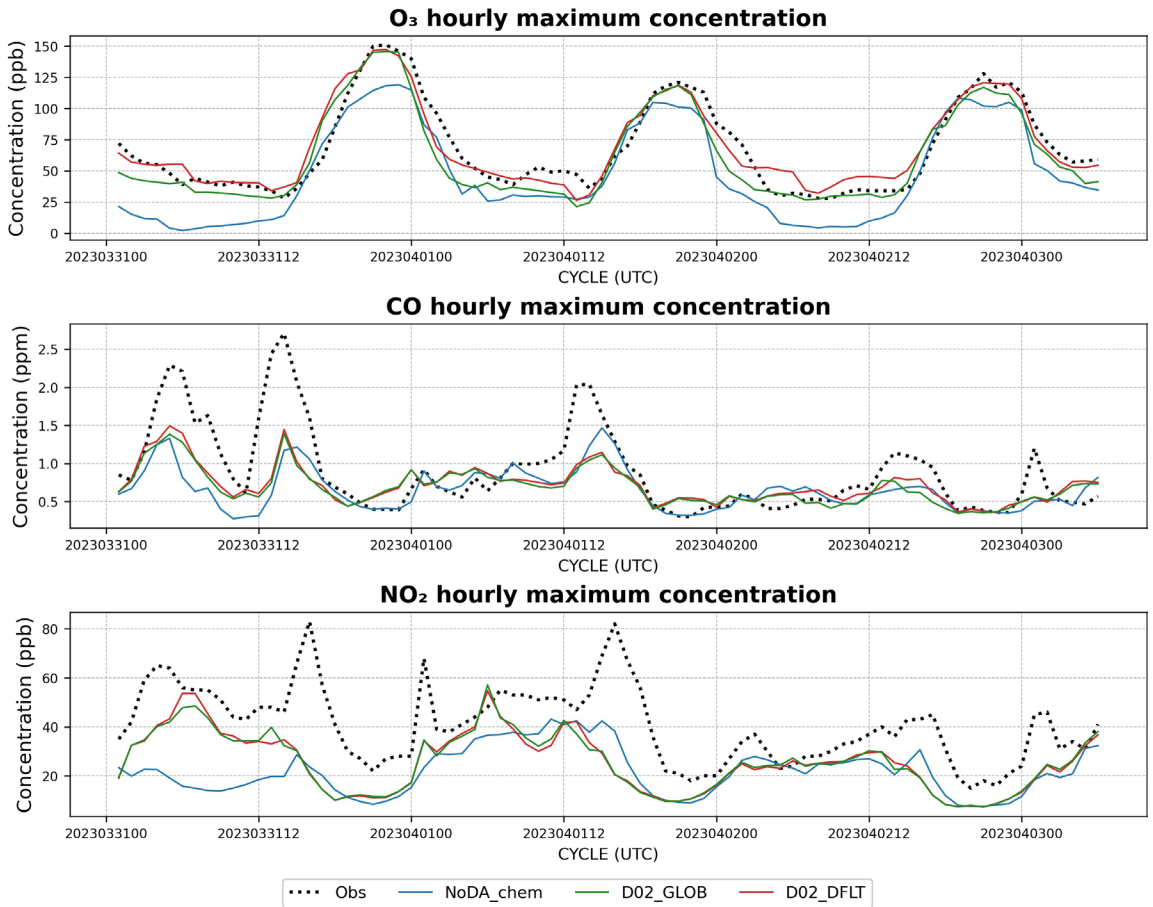

Figure 11. Time series of O_3, CO and NO_2 comparing observed (dots) and modeled hourly regional maximum concentrations for the NoDA_chem (blue), D02_GLOB (green) and D02_DFLT (red) experiments.

for NO_2, even though the assimilation process improved model concentrations during the first 14 hours of March 31st and during the April 1st 06:00 UTC cycle, the model showed a tendency to underestimate the concentrations of this pollutant after several cycles. As previously mentioned, the assimilation of more meteorological variables could help improve model performance because of the impact that meteorology has on the transport of pollutants.

Table 3 illustrates the statistical metrics estimated using the hourly regional maximum values. It shows that the model performance improves significantly when estimating ozone maximum concentration, particularly in the D02_GLOB experiment. For CO and NO_2, however, no improvements were observed in pollutant concentrations estimation. Regarding meteorology, the model's performance shows significant enhancement compared to the statistical metrics calculated using the regional hourly average (Table 2).

These results suggest that using the initial and boundary conditions from a global model was more effective for estimating regional maximum ozone concentrations during the day. However, the modeled peak ozone concentrations were very similar when using global and default initial conditions.

Furthermore, additional research on the impact of using different tuning parameters (horizontal and vertical scaling) for the background error covariance matrix (**B**) is required. In this sense, future investigations will discuss the impact of estimating **B** using 24-48 hours forecasts valid at the same time instead of 12-24 hours and the effect of employing a longer period for its calculation (for example, several months). This will allow us to increase our understanding about the specific conditions under which a static background error covariance matrix could lead to an improved assimilation quality and therefore model performance.

4. Conclusions

This work presents one of the first efforts to improve the estimation of pollutant concentrations using chemical data assimilation in México. We analyzed the sensitivity of the WRF-DA-Chem assimilation system to different initial and boundary conditions when surface observations were assimilated.

The observation minus analysis (OMA) and observation minus background (OMB) statistics showed differences between the data assimilation (DA) experiments. For example, root mean square error (RMSE) decreased for ozone in both DA experiments and was slightly higher for the global chemical conditions (D02_GLOB case). For carbon monoxide (CO) and nitrogen dioxide (NO_2), OMB RMSE decreased in some cycles when the observations were assimilated in both DA experiments but remained similar in others. This may be related to an insufficiently accurate representation of meteorological variables during these

Table 3. Statistical metrics using hourly regional maximum concentrations for NoDA_chem, D02_DFLT and D02_GLOB experiments.

		NoDA_chem	D02_DFLT	D02_GLOB
O_3	d	0.73	0.84	0.90
	RMSE	20.24	12.32	8.20
	Pearson	0.96	0.98	0.98
CO	d	0.60	0.60	0.66
	RMSE	0.53	0.50	0.46
	Pearson	0.70	0.70	0.71
NO_2	d	0.13	0.13	0.15
	RMSE	23.97	24.99	24.76
	Pearson	0.70	0.56	0.57
T	d	0.80	0.81	0.81
	RMSE	2.40	2.13	2.12
	Pearson	0.98	0.98	0.98
RH	d	0.88	0.72	0.72
	RMSE	6.78	15.18	15.19
	Pearson	0.97	0.97	0.97
U	d	0.42	0.48	0.47
	RMSE	1.62	1.36	1.36
	Pearson	0.17	0.59	0.59
V	d	0.56	0.79	0.78
	RMSE	1.21	0.61	0.62
	Pearson	0.64	0.91	0.91

cycles, since the reduced impact observed in these experiments may be related to an insufficiently accurate representation of meteorological variables during the assimilation cycles, because no clear sensitivity to boundary conditions was identified. Although meteorological initial conditions can be improved with data assimilation, uncertainties in key processes, in particular wind fields and planetary boundary layer height, might determine the improvement of chemical forecasts, and systematic errors that affect chemical transport and reactive processes might not be fully reduced (Cho *et al.*, 2025; Zhang *et al.*, 2012).

Regarding the average increments, their magnitudes exceeded 5 ppb for O_3, 15 ppb for NO_2 and over 0.3 ppm for CO. However, the absence of a clear reflection of the analysis increments in modeled concentrations at 00:00 UTC is consistent with known limitations of data assimilation in coupled meteorology–chemistry models based on 3DVAR, where the analysis increments are applied only at the initial assimilation time and are heavily dependent on the prescribed background error covariance matrix, since if the length scales are not adequately representing the true error structures of meteorological variables relevant for chemical transport, the resulting increments might be not enough to modify the large-scale flow patterns that impact pollutants transport and their spatial distribution (Descombes *et al.*, 2015). Therefore, at 00:00 UTC (immediately after the analysis), the model might need an additional integration time for the meteorological increments to have an effect on chemical composition. This has been reported in previous studies using this data assimilation system, where the impact of data assimilation on chemical fields is more evident at short forecast lead times rather than at the initial assimilation time (Ha, 2022).

With respect to model evaluation, the performance in estimating ozone concentration improved in both assimilation experiments compared to the case without data assimilation in terms of the statistical metrics. For CO and NO_2, assimilation experiments generally missed observed values during peak concentration hours, though improvements were seen in early assimilation cycles compared to the control case. Differences between D02_DFLT and D02_GLOB experiments for these pollutants were minor, likely due to the need of additional tuning of the background error covariance matrix assimilation parameters (variance, length scale, among others). Furthermore, the assimilation of meteorological variables in the inner domain could enhance model performance for chemical species by improving meteorological fields in MCMA.

The results also suggested that using global model outputs as initial and boundary conditions for the larger domain led to a small increase in hourly regional average ozone concentrations and tended to perform best for estimating hourly regional maximum concentrations. However, in terms of daily peak ozone values, there was no clear difference of using a global model over using a default profile for boundary conditions. This is important, because computational resources costs for both storage and processing may be reduced and optimized if solving the chemistry only at the regional level. Thus, a workflow of solving first the meteorology at the synoptic scale and then solving the chemistry at the regional level might be better for optimizing limited resources. In this regard, a longer cycled experiment using the default chemical conditions can result in more frequent initializations and thus in an improved and spun up chemical conditions.

Statistical metrics for meteorological fields show minor changes between the DA experiments and the control case. This indicates that the control run is already providing a reasonable representation of the atmospheric state, and that data assimilation is resulting more in fine adjustments to the initial conditions rather than large corrections, which may not be captured by aggregated metrics such as RMSE or correlation (Zou, 2025). Thus, these small changes in meteorological metrics are suggesting a more localized correction to the atmospheric state by the assimilation process.

Future work will address surface-level meteorological data assimilation using observations that are not included in the global meteorological data set, as well as the tuning of the assimilations system parameters associated with background error with the aim of constructing tools to support stakeholders during pollution episodes in the MCMA.

5. Acknowledgements

The authors acknowledge the Comision Ambiental de la Megalópolis (CAMe) for the resources provided to conduct this study through proyect "*Ensamble para alerta temprana de episodios y pronóstico de calidad del aire. Componente 1. Asimilación de datos de química atmosférica y meteorológicos para la región de la Megalópolis*".

6. References

Ahmadov, R., McKeen, S. A., Robinson, A. L., Bahreini, R., Middlebrook, A. M., de Gouw, J. A., Meagher, J., Hsie, E. -Y., Edgerton, E., Shaw, S., & Trainer, M. (2012). A volatility basis set model for summertime secondary organic aerosols over the eastern United States in 2006. *Journal of Geophysical Research: Atmospheres, 117*(D6). **https://doi.org/10.1029/2011jd016831**

Aleksankina, K., Reis, S., Vieno, M., & Heal, M. R. (2019). Advanced methods for uncertainty assessment and global sensitivity analysis of an Eulerian atmospheric chemistry transport model. *Atmospheric*

Chemistry and Physics, 19(5), 2881–2898. https://doi.org/10.5194/acp-19-2881-2019

Baklanov, A., & Zhang, Y. (2020). Advances in air quality modeling and forecasting. *Global Transitions, 2*, 261–270. https://doi.org/10.1016/j.glt.2020.11.001

Ban, J., Liu, Z., Zhang, X., Huang, X. Y., & Wang, H. (2017). Precipitation data assimilation in WRFDA 4D-Var: Implementation and application to convection-permitting forecasts over United States. *Tellus, Series A: Dynamic Meteorology and Oceanography, 69*(1). https://doi.org/10.1080/16000870.2017.1368310

Barker, D., Huang, X. Y., Liu, Z., Auligné, T., Zhang, X., Rugg, S., Ajjaji, R., Bourgeois, A., Bray, J., Chen, Y. E., Demirtas, M., Guo, Y. R., Henderson, T., Huang, W., Lin, H. C., Michalakes, J., Rizvi, S., & Zhang, X. (2012). The weather research and forecasting model's community variational/ensemble data assimilation system: WRFDA. *Bulletin of the American Meteorological Society, 93*(6), 831–843. https://doi.org/10.1175/BAMS-D-11-00167.1

Bei, N., de Foy, B., Lei, W., Zavala, M., & Molina, L. T. (2008). Using a 3D-variational data assimilation system to improve ozone simulations in the Mexico City basin. *Atmospheric Chemistry and Physics, 8*(24), 7353–7365. https://doi.org/10.5194/acp-8-7353-2008

Bei, N., Lei, W., Zavala, M., & Molina, L. T. (2010). Ozone predictabilities due to meteorological uncertainties in the Mexico City basin using ensemble forecasts. *Atmospheric Chemistry and Physics, 10*(13), 6295–6309. https://doi.org/10.5194/acp-10-6295-2010

Bei, N., Li, G., & Molina, L. T. (2012). Uncertainties in SOA simulations due to meteorological uncertainties in Mexico City during MILAGRO-2006 field campaign. *Atmospheric Chemistry and Physics, 12*(23), 11295–11308. https://doi.org/10.5194/acp-12-11295-2012

Bei, N., Li, G., Meng, Z., Weng, Y., Zavala, M., & Molina, L. T. (2014). Impacts of using an ensemble Kalman filter on air quality simulations along the California-Mexico border region during Cal-Mex 2010 field campaign. *The Science of the Total Environment, 499*, 141–153. https://doi.org/10.1016/j.scitotenv.2014.07.121

Bocquet, M., Elbern, H., Eskes, H., Hirtl, M., Aabkar, R., Carmichael, G. R., Flemming, J., Inness, A., Pagowski, M., Pérez Camaño, J. L., Saide, P. E., San Jose, R., Sofiev, M., Vira, J., Baklanov, A., Carnevale, C., Grell, G., & Seigneur, C. (2015). Data assimilation in atmospheric chemistry models: Current status and future prospects for coupled chemistry meteorology models. *Atmospheric Chemistry and Physics, 15*(10), 5325–5358. https://doi.org/10.5194/acp-15-5325-2015

Chin, M., Rood, R. B., Lin, S. J., Müller, J. F., & Thompson, A. M. (2000). Atmospheric sulfur cycle simulated in the global model GOCART: Model description and global properties. *Journal of Geophysical Research: Atmospheres, 105*(D20), 24671–24687. https://doi.org/10.1029/2000JD900384

Cho, Y., Kim, H. M., Seo, M. G., & Kim, D. H. (2025). Effects of chemical and meteorological data assimilation on air-quality and meteorological forecasts in the Korean Peninsula. *The Science of the Total Environment, 990*, 179842. https://doi.org/10.1016/j.scitotenv.2025.179842

Comisión Nacional del Agua. (2024). *Reporte anual del clima en México 2023* (Año 13, Número 13).

Comisión Nacional Forestal. (2024). *Cierre Estadístico 2023*. Recuperado el 3 de enero de 2025, de https://www.gob.mx/cms/uploads/attachment/file/879026/

Davis, B., Wang, X., & Lu, X. (2021). A comparison of HWRF Six-Hourly 4DEnVar and Hourly 3DEnVar assimilation of inner core tail doppler radar observations for the prediction of hurricane Edouard (2014). *Atmosphere, 12*(8), 942. https://doi.org/10.3390/atmos12080942

Descombes, G., Auligné, T., Vandenberghe, F., Barker, D. M., & Barré, J. (2015). Generalized background error covariance matrix model (GEN-BE v2.0). *Geoscientific Model Development, 8*(3), 669–696. https://doi.org/10.5194/gmd-8-669-2015

García-Reynoso, J. A., Mar-Morales, B. E., & Ruiz-Suárez, L. G. (2018). Spatial, temporal and speciation model of the Mexico national emissions inventory (base year 2008) for its use in air quality modeling (DiETE). *Revista Internacional de Contaminación Ambiental, 34*(4), 635–649. https://doi.org/10.20937/RICA.2018.34.04.07

Gelaro, R., McCarty, W., Suárez, M. J., Todling, R., Molod, A., Takacs, L., Randles, C. A., Darmenov, A., Bosilovich, M. G., Reichle, R., Wargan, K., Coy, L., Cullather, R., Draper, C., Akella, S., Buchard, V., Conaty, A., da Silva, A. M., Gu, W., … Zhao, B. (2017). The modern-era retrospective analysis for research and applications, version 2 (MERRA-2). *Journal of Climate, 30*(14), 5419–5454. https://doi.org/10.1175/JCLI-D-16-0758.1

Grell, G. A. (1993). Prognostic evaluation of assumptions used by cumulus parameterizations. *Monthly Weather Review, 121*(3), 764-787. https://doi.org/10.1175/1520-0493(1993)121<0764:PEOAUB>2.0.CO;2

Grell, G. A., & Dévényi, D. (2002). A generalized approach to parameterizing convection combining ensemble and data assimilation techniques. *Geophysical Research Letters, 29*(14), 1693. https://doi.org/10.1029/2002GL015311

Grell, G., Peckham, S. E., Schmitz, R., McKeen, S. A., Frost, G., Skamarock, W. C., & Eder, B. (2005). Fully coupled "online" chemistry within the WRF model. *Atmospheric Environment, 39*(37), 6957–6975. https://doi.org/10.1016/j.atmosenv.2005.04.027

Ha, S. (2022). Implementation of aerosol data assimilation in WRFDA (v4.0.3) for WRF-Chem (v3.9.1) using the RACM/MADE-VBS scheme. *Geoscientific Model Development, 15*(4), 1769–1788. https://doi.org/10.5194/gmd-15-1769-2022

Ha, S., Kumar, R., Pfister, G., Lee, Y., Lee, D., Kim, H. M., & Ryu, Y. H. (2024). Chemical data assimilation with aqueous chemistry in WRF-Chem coupled with WRFDA (V4.4.1). *Journal of Advances in Modeling Earth Systems, 16*(2), e2023MS003928. https://doi.org/10.1029/2023MS003928

Hong, S. Y., & Lim, J. O. J. (2006). The WRF single-moment 6-class microphysics scheme (WSM6). *Journal of the Korean Meteorological Society, 42*(2), 129-151.

Hong, S. Y., Noh, Y., & Dudhia, J. (2006). A new vertical diffusion package with an explicit treatment of entrainment processes. *Monthly Weather Review, 134*(9), 2318-2341. **https://doi.org/10.1175/mwr3199.1**

Huang, X. Y., Xiao, Q., Barker, D. M., Zhang, X., Michalakes, J., Huang, W., Henderson, T., Bray, J., Chen, Y., Ma, Z., Dudhia, J., Guo, Y., Zhang, X., Won, D. J., Lin, H. C., & Kuo, Y. H. (2009). Four-dimensional variational data assimilation for WRF: Formulation and preliminary results. *Monthly Weather Review, 137*(1), 299–314. **https://doi.org/10.1175/2008MWR2577.1**

Iacono, M. J., Delamere, J. S., Mlawer, E. J., Shephard, M. W., Clough, S. A., & Collins, W. D. (2008). Radiative forcing by long-lived greenhouse gases: Calculations with the AER radiative transfer models. *Journal of Geophysical Research: Atmospheres, 113*(13), D13103. **https://doi.org/10.1029/2008JD009944**

Instituto Nacional de Ecología y Cambio Climático. (2020). *Informe Nacional de la Calidad del Aire 2019, México*.

Instituto Nacional de Ecología y Cambio Climático. (2024). *Informe Nacional de la Calidad del Aire 2021, México*.

Lee, M., & Barker, D. (2005). Preliminary tests of First Guess at Appropriate Time (FGAT) with WRF 3DVAR and WRF model. *Journal of the Korean Meteorological Society, 41*(4), 495-505.

Lei, W., de Foy, B., Zavala, M., Volkamer, R., & Molina, L. T. (2007). Characterizing ozone production in the Mexico City Metropolitan Area: A case study using a chemical transport model. *Atmospheric Chemistry and Physics, 7*(5), 1347–1366. **https://doi.org/10.5194/acp-7-1347-2007**

López-Espinoza, E. D., Zavala-Hidalgo, J., & Gómez-Ramos, O. (2012). Weather forecast sensitivity to changes in urban land covers using the WRF model for central México. *Atmósfera, 25*(2), 127-154.

Mallet, V., & Sportisse, B. (2006). Uncertainty in a chemistry-transport model due to physical parameterizations and numerical approximations: An ensemble approach applied to ozone modeling. *Journal of Geophysical Research: Atmospheres, 111*(1), D01302. **https://doi.org/10.1029/2005JD006149**

Martínez-Sabari, E. E., & García-Reynoso, J. A. (2021). Meteorological data assimilation for air quality modeling with WRF-Chem: Central Mexico case study. *Atmósfera, 34*(3), 311–336. **https://doi.org/10.20937/ATM.52804**

McKeen, S. A., Wotawa, G., Parrish, D. D., Holloway, J. S., Buhr, M. P., Hübler, G., Fehsenfeld, F. C., & Meagher, J. F. (2002). Ozone production from Canadian wildfires during June and July of 1995. *Journal of Geophysical Research: Atmospheres, 107*(D14), 4193. **https://doi.org/10.1029/2001JD000697**

Milan, M., Macpherson, B., Tubbs, R., Dow, G., Inverarity, G., Mittermaier, M., Halloran, G., Kelly, G., Li, D., Maycock, A., Payne, T., Piccolo, C., Stewart, L., & Wlasak, M. (2020). Hourly 4D-Var in the Met Office UKV operational forecast model. *Quarterly Journal of the Royal Meteorological Society, 146*(728), 1281–1301. **https://doi.org/10.1002/QJ.3737**

Mizzi, A. P., Arellano, A. F., Edwards, D. P., Anderson, J. L., & Pfister, G. G. (2016). Assimilating compact phase space retrievals of atmospheric composition with WRF-Chem/DART: A regional chemical transport/ensemble Kalman filter data assimilation system. *Geoscientific Model Development, 9*(3), 965–978. **https://doi.org/10.5194/gmd-9-965-2016**

Molina, L. T., Retama, A., & Zavala, M. (2023). *Diagnosis of current knowledge of the scientific bases for air quality management in the Megalopolis*. Molina Center for Strategic Studies in Energy and the Environment. **https://www.gob.mx/cms/uploads/attachment/file/869816/Diagnostic_Report__full_version_.pdf**

National Centers for Environmental Prediction. (2008). *NCEP ADP global upper air and surface weather observations (PREPBUFR format)* [Dataset]. NSF National Center for Atmospheric Research. Recuperado el 12 de febrero de 2025, de **https://gdex.ucar.edu/datasets/d337000/citation/**

https://doi.org/10.5065/Z83F-N512

National Centers for Environmental Prediction. (2015). NCEP GFS 0.25 Degree Global Forecast Grids Historical Archive [Dataset]. NSF National Center for Atmospheric Research. Recuperado el 10 de febrero de 2025, de **https://gdex.ucar.edu/datasets/d084001/citation/**

https://doi.org/10.5065/D65D8PWK

Parrish, D. F., & Derber, J. C. (1992). The National Meteorological Center's spectral statistical-interpolation analysis system. *Monthly Weather Review, 120*(8), 1747-1763. **https://doi.org/10.1175/1520-0493(1992)120<1747:TNMCSS>2.0.CO;2**

Peuch, V. H., Engelen, R., Rixen, M., Dee, D., Flemming, J., Suttie, M., Ades, M., Agustí-Panared, A., Ananasso, C., Andersson, E., Armstrong, D., Barré, J., Bousserez, N., Dominguez, J. J., Garrigues, S., Inness, A., Jones, L., Kipling, Z., Letertre-Dancza, J., … Thépaut, J. N. (2022). The Copernicus Atmosphere Monitoring Service from research to operations. *Bulletin of the American Meteorological Society, 103*(12), E2650–E2668. **https://doi.org/10.1175/BAMS-D-21-0314.1**

Risanto, C. B., Castro, C. L., Arellano, A. F., Moker, J. M., & Adams, D. K. (2021). The impact of assimilating gps precipitable water vapor in convective-permitting wrf-arw on north american monsoon precipitation forecasts over northwest mexico. *Monthly Weather Review, 149*(9), 3013–3035. **https://doi.org/10.1175/MWR-D-20-0394.1**

Saide, P. E., Kim, J., Song, C. H., Choi, M., Cheng, Y., & Carmichael, G. R. (2014). Assimilation of next generation geostationary aerosol optical depth retrievals to improve air quality simulations. *Geophysical Research Letters, 41*(24), 9188–9196. **https://doi.org/10.1002/2014GL062089**

Secretaría de Medio Ambiente y Recursos Naturales. (2019). *Inventario Nacional de Emisiones 2016*.

Secretaría del Medio Ambiente de la Ciudad de México. (2025). *Monitoreo de Contaminantes Criterio*. Recuperado el 1 de febrero de 2025, de **http://www.aire.cdmx.gob.mx/**

Stockwell, W. R., Kirchner, F., Kuhn, M., & Seefeld, S. (1997). A new

mechanism for regional atmospheric chemistry modeling. *Journal of Geophysical Research: Atmospheres, 102*(D22), 25847-25879. **https://doi.org/10.1029/97jd00849**

Sun, W., Liu, Z., Chen, D., Zhao, P., & Chen, M. (2020). Development and application of the WRFDA-Chem three-dimensional variational (3DVAR) system: Aiming to improve air quality forecasting and diagnose model deficiencies. *Atmospheric Chemistry and Physics, 20*(15), 9311–9329. **https://doi.org/10.5194/acp-20-9311-2020**

Vendrasco, E. P., Sun, J., Herdies, D. L., & de Angelis, C. F. (2016). Constraining a 3DVAR radar data assimilation system with large-scale analysis to improve short-range precipitation forecasts. *Journal of Applied Meteorology and Climatology, 55*(3), 673–690. **https://doi.org/10.1175/JAMC-D-15-0010.1**

West, J. J., Zavala, M. A., Molina, L. T., Molina, M. J., San Martini, F., McRae, G. J., Sosa-Iglesias, G., & Arriaga-Colina, J. L. (2004). Modeling ozone photochemistry and evaluation of hydrocarbon emissions in the Mexico City metropolitan area. *Journal of Geophysical Research: Atmospheres, 109*(D19), D19312. **https://doi.org/10.1029/2004JD004614**

Willmott, C. J., Ackleson, S. G., Davis, R. E., Feddema, J. J., Klink, K. M., Legates, D. R., O'Donnell, J., & Rowe, C. M. (1985). Statistics for the evaluation and comparison of models. *Journal of Geophysical Research: Oceans, 90*(C5), 8995–9005. **https://doi.org/10.1029/JC090iC05p08995**

World Health Organization, United Nations Children's Fund, United Nations Development Programme & United Nations Environment Programme (2024). Air pollution (Chap. 2). In *Compendium of WHO and other UN guidance in health and environment, 2024 update*. World Health Organization. **https://iris.who.int/handle/10665/378095**

Yang, C., Liu, Z., Gao, F., Childs, P. P., & Min, J. (2017). Impact of assimilating GOES imager clear-sky radiance with a rapid refresh assimilation system for convection-permitting forecast over Mexico. *Journal of Geophysical Research: Atmospheres, 122*(10), 5472–5490. **https://doi.org/10.1002/2016JD026436**

Yang, Y., & Wang, X. (2024). A comparison of 3DEnVar and 4DEnVar for convective-scale direct radar reflectivity data assimilation in the context of a filter and a smoother. *Monthly Weather Review, 152*(1), 59–78. **https://doi.org/10.1175/MWR-D-23-0082.1**

Zängl, G., Reinert, D., Rípodas, P., & Baldauf, M. (2015). The ICON (ICOsahedral Non-hydrostatic) modelling framework of DWD and MPI-M: Description of the non-hydrostatic dynamical core. *Quarterly Journal of the Royal Meteorological Society, 141*(687), 563–579. **https://doi.org/10.1002/QJ.2378**

Zaveri, R. A., Easter, R. C., Fast, J. D., & Peters, L. K. (2008). Model for Simulating Aerosol Interactions and Chemistry (MOSAIC). *Journal of Geophysical Research: Atmospheres, 113*(D13), D13204. **https://doi.org/10.1029/2007JD008782**

Zhang, Y., Bocquet, M., Mallet, V., Seigneur, C., & Baklanov, A. (2012). Real-time air quality forecasting, part I: History, techniques, and current status. *Atmospheric Environment, 60*, 632–655. **https://doi.org/10.1016/j.atmosenv.2012.06.031**

Zou, X. (2025). Traditional data assimilation and its effective integration with meteorological deep learning. *Engineering, 146*(730), 1999–2049. **https://doi.org/10.1016/j.eng.2025.11.023**